*Publications*

*DOE Grant No. DE-FG03-87-ER60513*

*Primcipal Invesitgator: Vincent McKoy*

# *Resonance Enhanced Multiphoton Ionization Spectra of Molecules and Molecular Fragments*

*Performance Period: March 1, 1990 - February 28, 1993*

We have used this iterative variational procedure to obtain the photoelectron wave functions needed in our studies of REMPI and single-photon ionization of molecules. This procedure and the associated computer programs have been fully implemented for linear molecules and some nonlinear systems such as $H_2O$, $CH_4$, and $C_2H_4$. Extension of these computer programs to polyatomic molecules of completely arbitrary geometry and implementation of these programs on *a massively parallel computer with over 6 gigabytes of memory are under way* and will be discussed in a later section of the proposal. The large memory and high-performance computing provided by these parallel computers will enable us to extend our studies to a wide range of polyatomic molecules.

## 3. *Summary of Progress* - 3/92 - 2/93 (FY 1993)

In this section I will review the progress we have made in our studies of ion rotational distributions resulting from resonance enhanced multiphoton ionization of excited electronic states and from single-photon ionization of ground electronic states of jet-cooled molecules by coherent VUV and XUV radiation. To do so I will select a few examples from our studies which serve to highlight our progress and to identify the background and significance of the specific spectral features and systems we have chosen to study.

### (a) *Resonance Enhanced Multiphoton Ionization of Molecules and Spectra*

As our first example we look at the rotational distributions of ions for (2+1) REMPI of the NH and OH radicals.[10,11] Fig. 1 shows (a) measured and (b) calculated rotationally resolved photoelectron spectra along with (c) calculated photoelectron angular distributions for (2 + 1) REMPI via the R(12) branch of the $f\ ^1\Pi(3p\sigma)$ state of NH for the $v^+ = 0$ and 1 levels of the ion. In these spectra the spin-orbit components of the $X\ ^2\Pi$ state of $NH^+$ and the parity components of the resonant and ionic states are not resolved. The calculated spectrum is also convoluted with a Gaussian detection function having a full-width at half-maximum (FWHM) of 30 meV. The most striking feature of these spectra is the appearance of strong $\Delta N = N^+ - N = even$ peaks, particularly for $\Delta N = 0$, for photoionization of this $3p\sigma$ Rydberg orbital of NH. On the basis of the simple selection rule $\Delta N + \ell = odd$,[11] these even $\Delta N(= 0, \pm 2)$ peaks must be associated with odd ($\ell = 1, 3$) angular momentum components of the photoelectron matrix element. With its 67% p character one would expect significant contributions from the $\ell = 0$ and 2 components of the photoelectron matrix element for ionization of this $3p\sigma$ Rydberg orbital.

## DISCLAIMER

## DISCLAIMER

Portions of this document may be illegible electronic image products. Images are produced from the best available original document.

It is clearly important to identify the underlying dynamical reason for the unusual behavior seen in these ion rotational distributions. Detailed calculations of these rotational

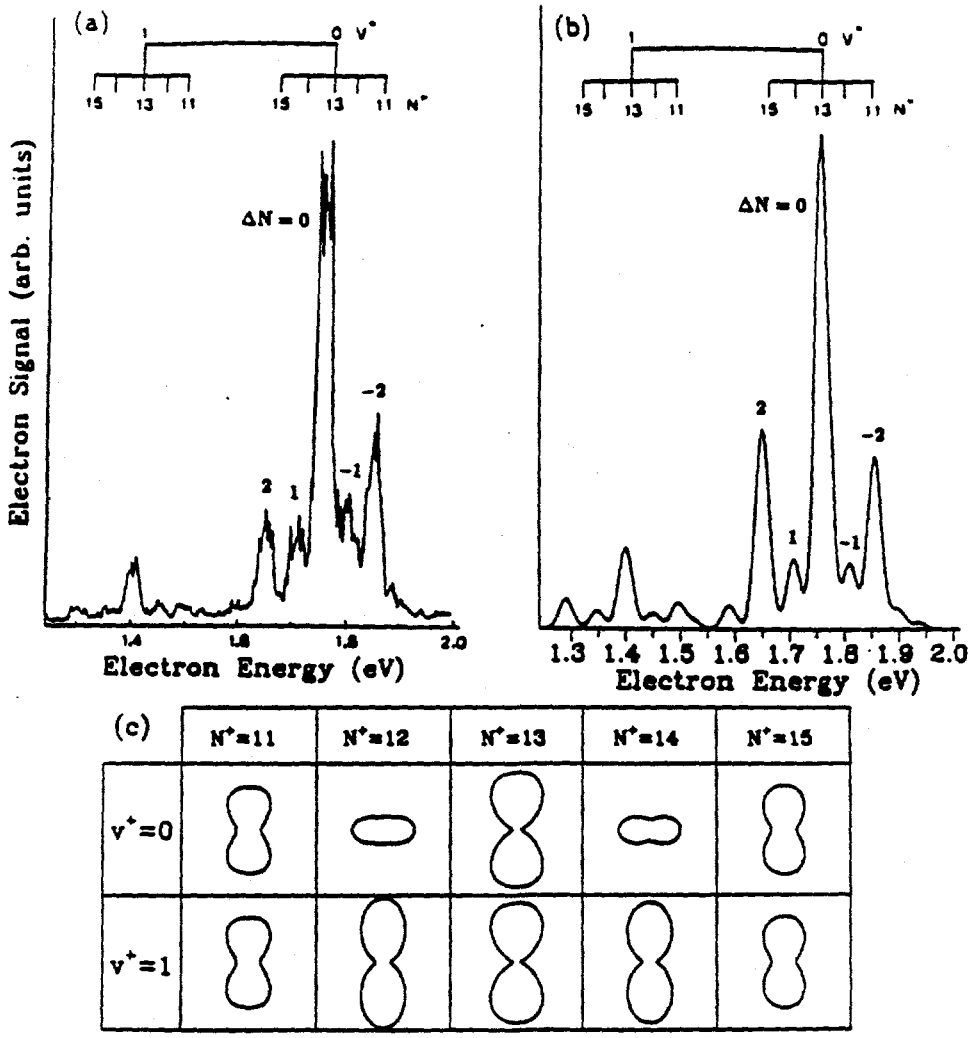


Fig. 1 (a) measured and (b) calculated photoelectron spectra along with the (c) calculated photoelectron angular distributions for (2 + 1) REMPI via the R(12) branch of the $f\ ^1\Pi(3p\sigma)$ state of NH for the $v^+ = 0$ and 1 vibrational bands. The measured spectra are taken from ref. 10.

distributions show that the strong even $\Delta N$ peaks in these spectra are, in fact, due to the presence of a Cooper minimum in the $\ell = 2$ component of the photoionization matrix element.[11] Such a Cooper minimum occurs at a photoelectron kinetic energy where a specific angular momentum component of the photoionization matrix element changes sign and goes through a zero. These angular momentum components of the photoelectron matrix element are essentially the driving force for ejection of the photoelectron with a

specific angular momentum $\ell$. At a Cooper minimum a specific $\ell$ component of this driving force is diminished and hence corresponding ion rotational peaks, which are related to $\ell$ through $\Delta N + \ell = odd$, are weakened. Here depletion of the d wave ($\ell = 2$) contributions to the photoelectron matrix element in the vicinity of the Cooper minimum weakens the $\Delta N$ = *odd* peaks and subsequently enhances the relative importance of the odd components ($\ell$ = 1 and 3) of this matrix element and, hence, that of the even $\Delta N$ rotational peaks.

Fig. 1 (c) shows the calculated photoelectron angular distributions for the ion rotational levels in the spectrum of fig. 1. A significant feature of these spectra is that the angular distributions for the $\Delta N = \pm 1$ peaks ($N^+ = 12$ and 14) are quite different for the $v^+ = 0$ and 1 levels of the ion. This behavior is due to a dependence of the photoelectron matrix element on internuclear distance which, in turn, arises from a rapid evolution of the $3p\sigma$ orbital of the $f\ ^1\Pi$ state from predominant 3p character at smaller internuclear distance to 3s character at larger R. It is surprising that this dependence is so evident for such low vibrational excitation.

Fig. 2 shows measured and calculated rotationally resolved photoelectron spectra for (2 + 1) REMPI of OH via the $O_{11}$ (11) branch of the $D\ ^2\Sigma^-(3p\sigma)$ [figs. 3(a) and 3(b)] and the $3\ ^2\Sigma^-(4s\sigma)$ [figs. 3(c) and 3(d)] Rydberg states.[12] These spectra again serve to demonstrate the significant influence that Cooper minima exert on ion rotational distributions. Cooper minima have been predicted to occur in the d ($\ell = 2$) wave of the $k\sigma$ and $k\pi$ continua for photoionization of the $D\ ^2\Sigma^-(3p\sigma)$ Rydberg state but not in the $3\ ^2\Sigma^-$ state. The presence of these Cooper minima for the $D\ ^2\Sigma^-$ state accounts for the occurence of strong $\Delta$ N = *even* signals in the photoelectron spectrum in contrast to the $\Delta$ N = *odd* distribution expected for ionization of a $3p\sigma$ Rydberg orbital in an atomiclike picture, i.e., $3p\sigma \rightarrow ks, kd$ photoionizing transitions. On the other hand, the photoelectron spectra for photoionization of the $3\ ^2\Sigma^-(4s\sigma)$ state of figs. 3(c) and 3(d) reveal a qualitatively different and much broader distribution with prominent $\Delta$ N = even and $\Delta$ N = odd transitions. The appearance of these spectra arises from greater $\ell$ - mixing in this higher Rydberg orbital (54% s and 43% p character at R = 2.043 $a_o$).

Cooper minima can be expected to have far-reaching and wide-spread implications for the behavior of ion rotational distributions. For example, similar effects in ion rotational distributions due to Cooper minima have also been predicted for $H_2O$ and SiF. Furthermore, Cooper minima can also be exploited to achieve a high degree of rotational selectivity in ion rotational distributions.[13]

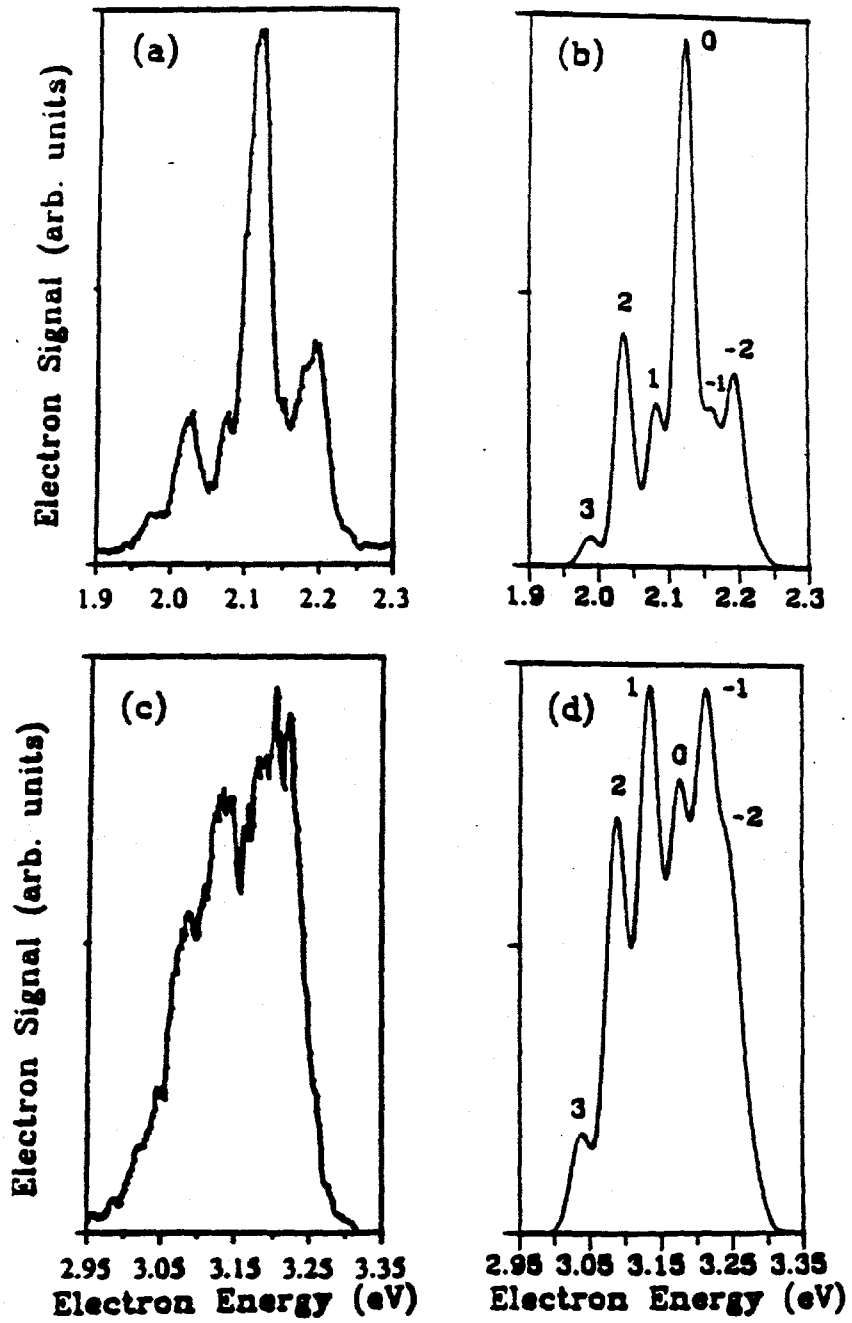


Fig. 2. Experimental and calculated rotationally resolved photoelectron spectra for (2 + 1) REMPI of OH: (a) measured spectrum for the $D\ ^2\Sigma^-(3p\sigma)$ state, $v = 0 \rightarrow v^+ = 0$, $O_{11}$ (11) rotational branch; (b) calculated $D\ ^2\Sigma^-$ photoelectron spectrum, assuming a Gaussian line shape with a FWHM of 30 meV; (c) measured spectrum for the $3\ ^2\Sigma^-(4s\sigma)$ state, $v' = 0 \rightarrow v^+ = 0$, $O_{11}$ (11) rotational branch; (d) calculated $3\ ^2\Sigma^-(4s\sigma)$

photoelectron spectrum assuming a Gaussian line shape with a FWHM of 35 meV. The labelling of peaks in the calculated spectra indicates the change of rotational quantum number $\Delta N = N^+ - N$.

We have also studied the rotational distributions of $HBr^+$ ions in their $X^2\Pi_{1/2}$ ground state for (2 + 1) REMPI of HBr via the S(2) branch of the F $^1\Delta_2$ ($5p\pi$) Rydberg state.[14] These studies were motivated by the recent measurements of Xie and Zare in which the

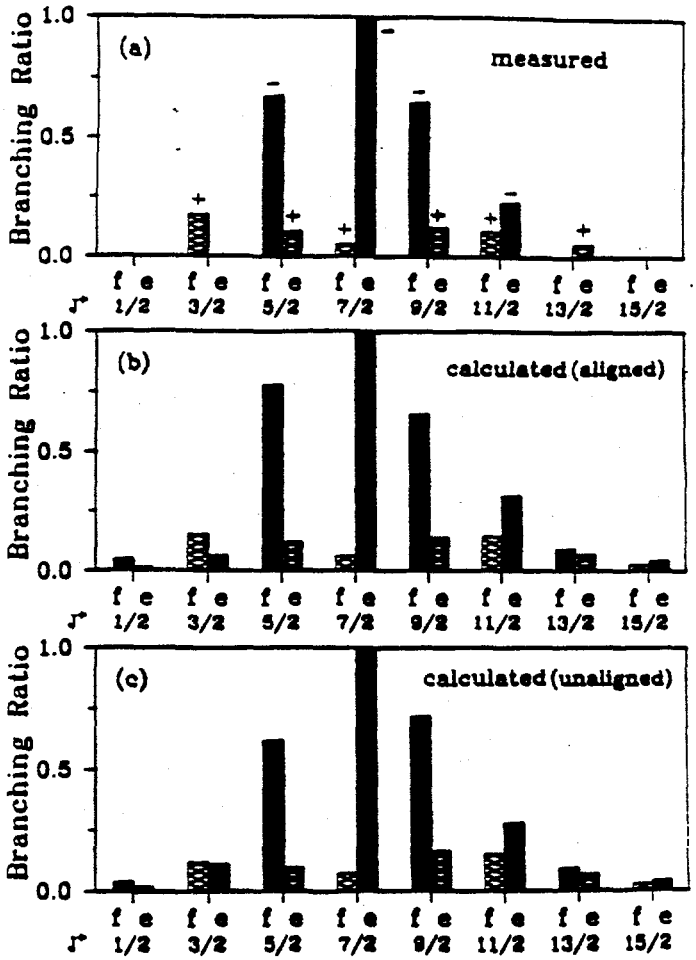


Fig. 3. Rotational distributions of $HBr^+$ for (2 + 1) REMPI via the S(2) branch of the F $^1\Delta_2$ state: (a) measured distributions of ref. 16; (b) and (c) calculated distributions for the unaligned and unaligned resonant states, respectively, of ref. 14.

populations of the individual parity components of each ion rotational level were obtained using laser-induced fluorescence.[15,16] Such measurements of ion populations for individual parity components of a $\Lambda$ doublet provide a very stringent test of the underlying angular momentum make-up of molecular photoelectron wavefunctions.[14,15] These spectra show

a strongly (−) parity-favored ion rotational distribution for photoionization of the (+) parity component of the J = 4 level of the $5p\pi$ Rydberg orbital of the $F^1\Delta_2$ state which has about 97% p ($\ell_0 = 1$) character. These (−) parity-favored ion distributions can be readily understood on the basis of parity selection rules[6,17] and the dominance of the photoelectron matrix element by its $\ell = 0$ and 2 angular momentum components for photoionization of this $5p\pi$ Rydberg orbital with its 97% p character. Fig. 3 compares our calculated ion rotational distributions with the measured spectra of Xie and Zare.[16] The photoelectron energy is about 2.33 eV. Calculated spectra are shown for photoionization of both the optically aligned J = 4 level (fig. 3(b)) and an unaligned J = 4 level (fig. 3(c)). The agreement between the calculated and measured ion distributions is very encouraging.

Note that, on the basis of parity selection rules,[6,17] the 20% population seen in the (+) parity component (cross-hatched bars) of the Λ doublet ***must be due to odd partial wave components of the photoelectron matrix element which arise from angular momentum coupling in the molecular photoelectron.*** Examination of the photoelectron matrix elements reveals that the f wave of the $5p\pi \rightarrow k\delta$ ionization channel makes the dominant contribution to the population of these (+) parity levels of the ion.[14] Such behavior is entirely nonatomic-like. Comparison of the ion distributions for the unaligned J = 4 level with those for an optically aligned J = 4 level and with the measured spectra serves to illustrate that, although not large, the effect of alignment can be important.

(b) *Threshold Photoionization of Linear Molecules*

We now highlight the progress we have made in our studies of ion rotational distributions for single-photon ionization of diatomic molecules and fragments by coherent VUV and XUV radiation. In contrast to the spectra discussed above where the photoelectron energies were of the order of 1 to 2 eV, we now look at ion rotational distributions for threshold photoionization where the photoelectron energy is essentially zero. The measured spectra with which our calculated ion rotational distributions will be compared in the two examples have been obtained using a technique based on the detection of zero-kinetic-energy (ZEKE) photoelectrons resulting from pulsed-field ionization (PFI) of very high Rydberg states lying below a rotational threshold.[5] This ZEKE-PFI technique makes it possible to obtain ion rovibronic state distributions with sub-wavenumber resolution. Although these ZEKE techniques are limited to measurements of threshold photoionization cross sections, this dramatic improvement in resolution over that of conventional photoelectron spectrometers certainly opens up new possibilities for studying photoionization dynamics, ion spectroscopy, and state-selected ion-molecule reactions. In fact, several novel applications built on the ultra-high resolution of this technique have already emerged.[18] Measurements

of ion rotational distributions for very low rotational levels and at threshold photoelectron energies, which this technique makes possible for a wide range of molecules, can certainly be expected to raise important theoretical challenges and to provide significant insight into the coupling of electronic and nuclear motion inherent in the photoionization process.

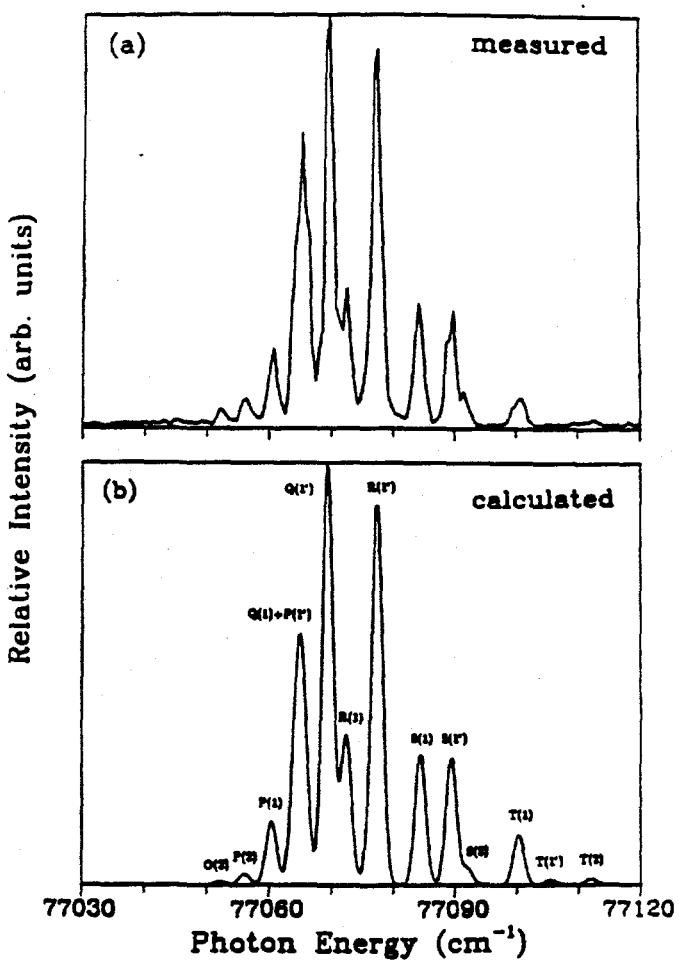


Fig. 4. (a) measured and (b) calculated ZEKE photoelectron spectra for single-photon ionization of rotationally cold NO (X $^2\Pi_{1/2}$) by coherent VUV radiation. The calculated spectrum is for 5 K

Fig. 4 shows the (a) measured and (b) our calculated ZEKE photoelectron spectra for single-photon ionization of rotationally cold NO (X $^2\Pi_{1/2}, v'' = 0$) molecules leading to $NO^+$ (X $^1\Sigma^+, v^+ = 1$) by coherent VUV radiation.[4] The calculated ion rotational distributions assume a temperature of 5 K. These spectra were calculated for a photoelectron energy of 50 meV and convoluted with a Gaussian detection function with a FWHM of 2 cm$^{-1}$. In this figure each branch is associated with a letter designation which refers only to the change in angular mementum apart from spin, i.e., $\Delta N = N^+ - N''$. The label 1'

denotes the $N'' = 1$, $J'' = 1/2$ level. The agreement between these measured and calculated spectra is excellent.

To provide further insight into the underlying dynamics of these threshold photoelectron spectra, fig. 5 (a) and (b) show measured and calculated ion rotational branching ratios for photoionization of the $N'' = 1$, $J'' = 3/2$ rotational level of the X $^2\Pi_{1/2}$ ground state of NO. The data of fig. 5 (a) is extracted from the measured photoelectron spectrum

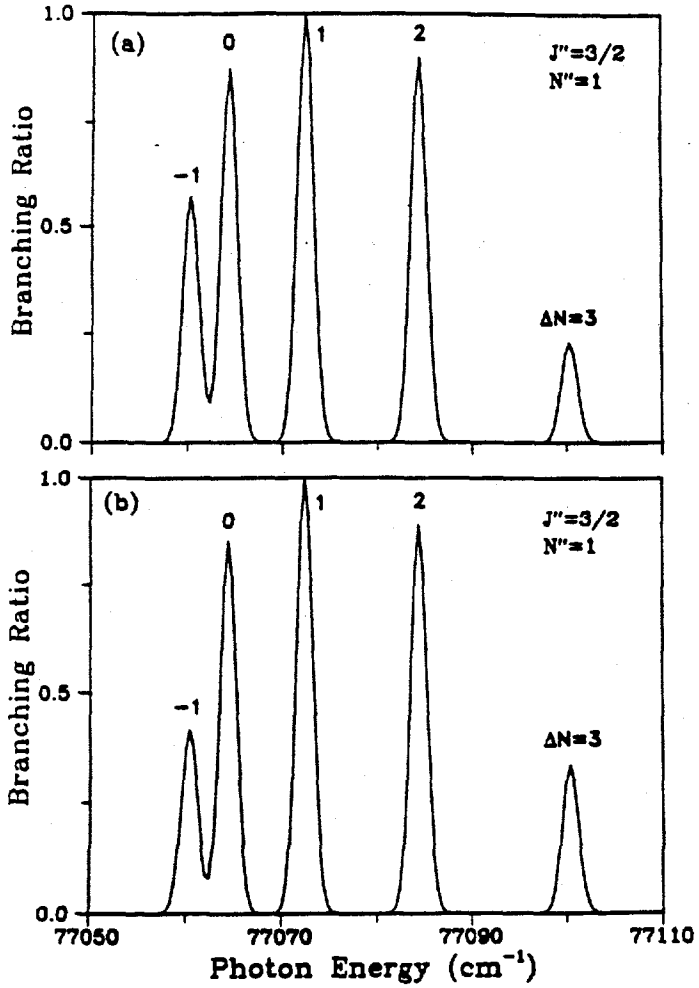


Fig. 5. (a) measured and (b) calculated ZEKE photoelectron spectra for single-photon ionization of the $N'' = 1$, $J'' = 3/2$ level of the $X^2\Pi_{1/2}$ state of NO by coherent VUV radiation.

of fig. 4 (a) for rotationally cold NO where, in addition to the $N'' = 1$ level, a few other rotational levels are also populated. These rotational branching ratios for ionization of this valence $2\pi$ orbital differ somewhat from those generally seen in ZEKE spectra of Rydberg states. This behavior reflects the broad range of angular momentum components ($\ell = 0$,

1, 2, and 3) which make significant contributions to the photoelectron matrix element for this valence orbital. Unusually strong s and d waves are predicted in addition to the p and f partial waves expected for photoionization of the $2\pi$ orbital with its 84% d ($\ell = 2$) character. These strong s and d components of the photoionization matrix element are due to angular momentum coupling in the molecular photoelectron wavefunction.

Fig. 6 shows the ZEKE photoelectron spectra for single-photon ionization of rotationally cold CO ($X\ ^1\Sigma^+$) molecules by coherent XUV radiation.[19] These jet-cooled PFI spectra

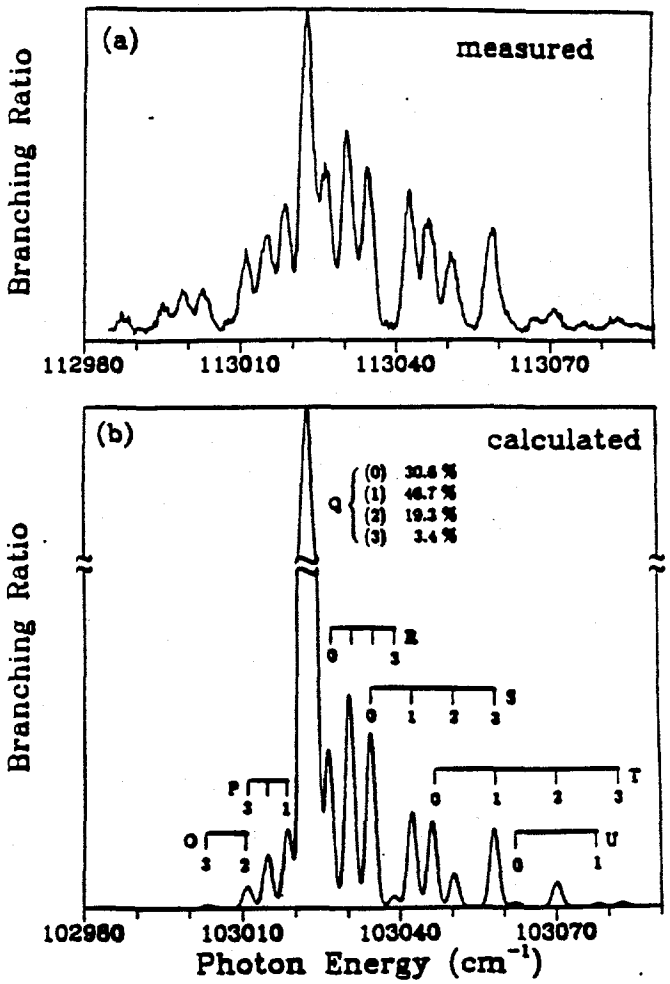


Fig. 6. (a) measured and (b) calculated ZEKE photoelectron spectra for single-photon ionization of rotationally cold CO ($X\ ^1\Sigma^+$) by coherent XUV radiation. The calculated spectrum is for 8 K.

are for the $v^+ = 0$ level of $CO^+(X\ ^2\Sigma^+)$. The calculated spectra assume a temperature of 8 K and a photoelectron energy of 50 meV and are convoluted with a Gaussian detection function with an FWHM of 2 cm$^{-1}$. The letter designation on each branch refers only to

the change of angular momentum apart from spin. The agreement between these calculated and measured rotational branching ratios is excellent for all branches except the Q($\Delta N = 0$) branch. This behavior is indicated by the broken scale in fig. 6 (b). The strength of the Q branches in these spectra is consistent with the parity selection rule, $\Delta N + \ell = \text{odd}$,[6] and the atomiclike behavior for photoionization of the $5\sigma$ orbital (45% s and 25% d character). The origin of this disagreement between these calculated and measured spectra is not yet clear.

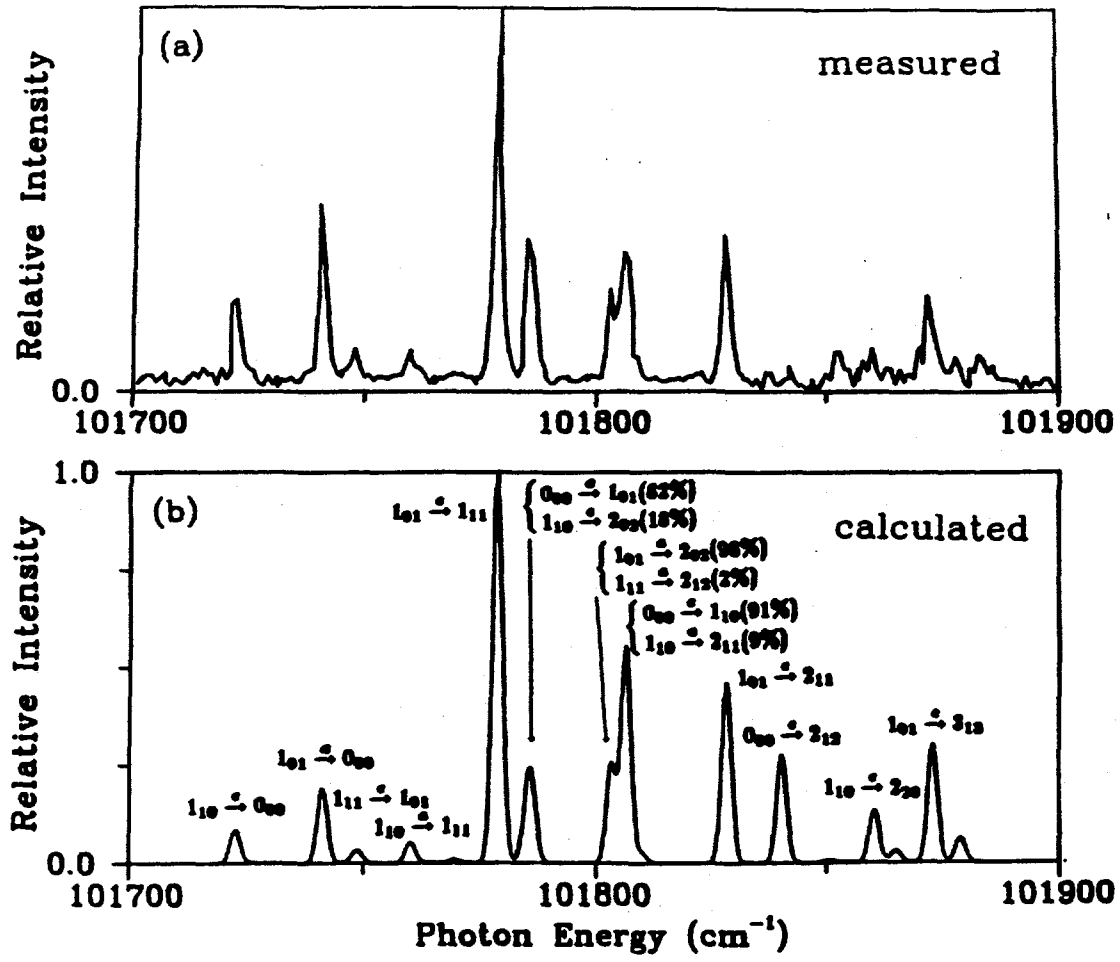


Fig. 7. (a) measured and (b) calculated ion rotational distributions for photoionization of the $1b_1$ orbital of the $\tilde{X}\ ^1A_1$ ground state of jet-cooled $H_2O$. The *a* and *c* labels indicate type *a* and type *c* transitions, respectively.

(c.) *Threshold Photoionization of Nonlinear Molecules*

Fig. 7 (a) shows the rotationally resolved ZEKE pulsed-field ionization spectrum of $H_2O$ recently reported by Tonkyn et al.[20] for single-photon ionization of the $1b_1$ orbital by coherent VUV radiation. This spectrum can be assigned to two types of rotational transitions, corresponding to specific changes in the asymmetric top angular momentum projection quantum numbers $K_a$ and $K_c$. Most of the strong spectral lines could be classified as type *c* rotational transitions ($\Delta K_a$ = even, $\Delta K_c$ = odd) are also clearly evident. Fig. 7 (b) shows our calculated ion rotational distributions[21] for photoionization of the $1b_1$ orbital of the $\tilde{X}\ ^1A_1$ ground state of jet-cooled $H_2O$ leading to the $\tilde{X}\ ^2B_1$ (000) state of the ion. A rotational temperature of 15 K is assumed in these calculations. Furthermore, we assume that there is no spin exchange taking place during the jet-cooled expansion of room-temperature water. The calculated spectrum is convoluted with a Gaussian detection function with a FWHM of 1.5 $cm^{-1}$. The agreement between the calculated and measured spectra is clearly encouraging except for the calculated $0_{00} \rightarrow 2_{12}$ transition which is somewhat stronger than that of the measured value.

The underlying dynamics of these photoelectron spectra is quite rich. We have shown that parity selection rules require that[7,21]

$$\Delta K_a + \ell = odd, \tag{13}$$

and

$$\mu + \lambda = \Delta K_b, \tag{14}$$

where $\mu$ is the photon polarization index in the molecular frame and $\lambda$ is the projection of $\ell$, the angular momentum of the photoelectron, in the molecular frame.[7] Eqs. (13) and (14) assume that the molecular z axis coincides with the $C_2$ symmetry axis and the x axis lies in the plane of the molecule. The molecular x, y, and z axis hence coincide with the a, c, and b axis, respectively. Since $\mu + \lambda$ is always odd for photoionization of the $1b_1$ orbital of $H_2O$, it can be shown that[7]

$$\Delta K_a + \Delta K_c = odd. \tag{15}$$

Both type *a* and type *c* transitions are allowed and type b [$\Delta K_a$ = even (odd) and $\Delta K_c$ = even (odd)] transitions are forbidden. Furthermore, eq. (13) shows that ***type a transitions*** ($1_{01} \rightarrow 0_{00}, 0_{00} \rightarrow 1_{01}, 1_{01} \rightarrow 2_{02}$, and $1_{11} \rightarrow 2_{12}$) ***arise from odd (almost pure p) wave contributions to the photoelectron matrix element.*** These p waves of the $ka_1$ and $kb_1$ continua are entirely molecular in origin since the almost p (99.7%) character of the $1b_1$ orbital of water leads only to s and d photoelectron continua in an atomiclike picture. The strong type *c* transitions in the spectra of fig. 7 arise from s and d (even) components of the photoelectron matrix element.

Figure 8 shows the (a) measured[22] and (b) our calculated[23] ion rotational distributions for single-photon ionization of the $2b_1$ orbital of the $\tilde{X}\,^1A_1$ (000) ground state of jet-cooled $H_2S$ by coherent VUV radiation leading to the $\tilde{X}\,^2B_1$ (000) ground state of the ion. These ion spectra are similar to those for the (000) level of $H_2O^+$ in fig. 7 in that threshold photoionization is accompanied by only small changes in total angular momentum

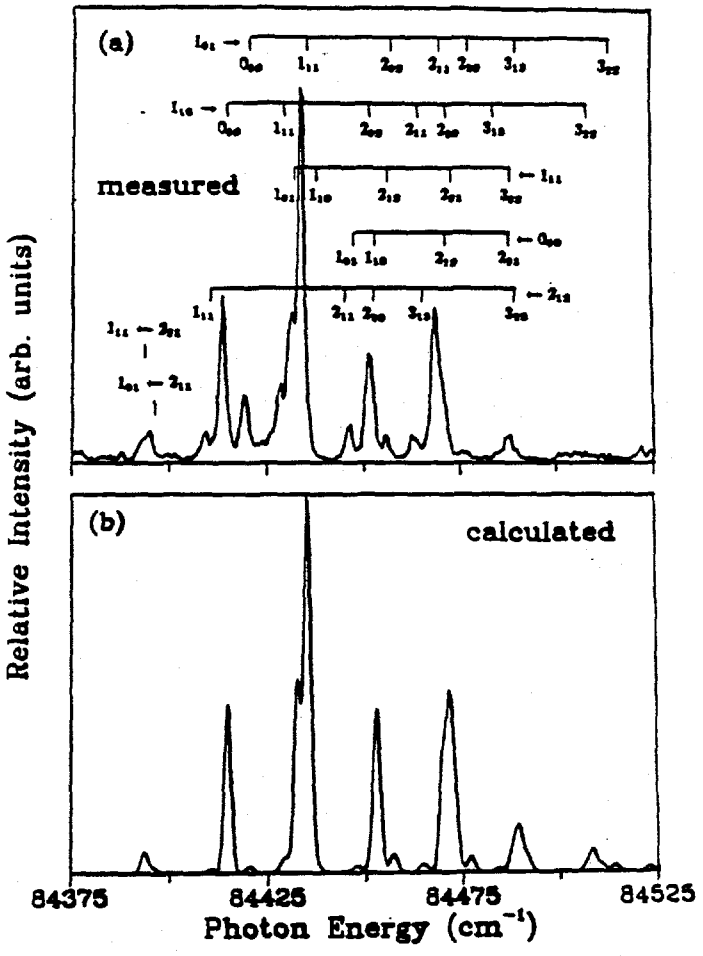


Fig. 8 (a) measured and (b) calculated ion rotational distributions for single-photon ionization of the $2b_1$ orbital of the $\tilde{X}^1A_1$ ground state of jet-cooled $H_2S$. The calculated spectrum is for 15 K and has an FWHM of 2 cm$^{-1}$

(excluding spin) $\Delta N$ and both type $c$ ($\Delta K_a = \pm 1, \Delta K_c = 0$) and type $a$ ($\Delta K_a = 0, \Delta K_c = \pm 1$) transitions are observed. The photoionization dynamics of the $2b_1$ orbital of $H_2S$ can be expected to be very similar to that of the $1b_1$ orbital of $H_2O$ since the $2b_1$ orbital is primarily localized on the sulfur atom and has about 99.8% p character. Furthermore, type $a$ transitons can also be expected to be weaker relative to type $c$ transitions in the photoelectron spectra of $H_2S$ than in $H_2O$ due to the more atomiclike character of $H_2S$.

In fact, a type *c* to type *a* intensity ratio of 4:1 is seen for photoionization of $H_2S$ in contrast to a 2:1 ratio for $H_2O$. The agreement between the calculated and measured spectra of fig. 8 is very encouraging even though the type *a* transiton ($1_{01} \rightarrow 0_{00}$) with negative $\Delta N$ is somewhat weaker in the calculated spectrum than observed. However, the type *a* transiton $1_{01} \rightarrow 2_{02}$ with $\Delta N = +1$ has almost the same intensity as seen in the measured spectrum. Note that the same photoelectron matrix elements are used in the calculation of the spectral intensities of these two type *a* transitions. This strongly suggests that the type *a* transition with negative $\Delta N$ is not due exclusively to direct ionization but probably involves autoionization. Such comparisions bwtween measured spectra and spectra calculated on the basis of direct ionization can clearly be helpful in clarifying the role of autoionization in these threshold photoelectron spectra.

d. *The research highlighted above have resulted in the following publications:*

1. *Rotationally resolved photoelectron spectra in resonance enhanced multiphoton ionization of Rydberg states of NH*
   K. Wang, J.A. Stephens, V. McKoy, E. de Beer,
   C.A. de Lange, and N.P.C. Westwood
   J. Chem. Phys. **97**, 211 (1992)

2. *Rotationally resolved photoelectron spectroscopy of the $^2\Sigma^-$ Rydberg states of OH. The role of Cooper minima*
   E. de Beer,C.A. de Lange, J.A. Stephens, K. Wang, and V. McKoy
   J. Chem. Phys. **95**, 714 (1992)

3. *Rotationally resolved threshold photoelectron spectra of OH and OD*
   R.T. Wiedmann, R.G. Tonkyn, M.G. White, K. Wang, and V. McKoy
   J. Chem. Phys. **97**, 768 (1992)

4. *Rotational branching ratios and photoelectron angular distributions in resonance enhanced multiphoton ionization of HBr via the $F^1\Delta_2$ Rydberg state*
   K. Wang and V. McKoy
   J. Chem. Phys. **95**, 7872 (1991)

5. *Rotationally resolved photoelectron spectra in resonance enhanced multiphoton ionization of HCl via the $F^1\Delta_2$ Rydberg state*
   K. Wang and V. McKoy
   J. Chem. Phys. **95**, 8718 (1991)

6. *Single-photon threshold photoionization of NO*

R.T. Wiedemann, M. G. White, K. Wang, and V. McKoy
J. Chem. Phys. (submitted for publication)

7. *Rotational state-selective photoionization dynamics of molecules at near-threshold photoelectron energies*
K. Wang, J.A. Stephens, and V. McKoy
J. Phys. Chem. (submitted as a *feature article*)

8. *Ion rotational distributions for near-threshold photoionization of $H_2O$*
M.-T. Lee, K. Wang, V. McKoy, R.G. Tonkyn,
R.T. Wiedmann, E.R. Grant, and M.G. White
J. Chem. Phys. **96**, 7848 (1992)

9. *Rotational resolved near-threshold photoionization of the $1b_1$ valence orbital of $H_2O$ and $D_2O$*
M.-T. Lee, K. Wang, and V. McKoy
J. Chem. Phys. **97**, 3108 (1992)

10. *Rotationally resolved photoelectron spectra in resonance enhanced multiphoton ionization of $H_2O$ via the $C\ ^1B_1$ Rydberg state*
M.-T. Lee, K. Wang, V. McKoy, and L.E. Machado
J. Chem. Phys. **97**, 3905 (1992)

11. *Rotationally resolved photoionization of molecular oxygen*
M. Braunstein, V. McKoy, and S.N. Dixit
J. Chem. Phys. **96**, 5726 (1992)

12. *Effects of Cooper minima in resonance enhanced multiphoton ionization-photoelectron spectroscopy of NO via the $D\ ^2\Sigma^+$ and $C\ ^2\Pi$ Rydberg states*
K. Wang, J.A. Stephens, and V. McKoy
J. Chem. Phys. **95**, 6456 (1991)

13. *Cooper minima and circular dichroism in photoelectron angular distributions*
H. Rudolph, R.L. Dubs, and V. McKoy
J. Chem. Phys. **93**, 7513 (1990)

14. *Non-Franck-Condon effects in photoionization of the $3\ ^3\Pi$ Rydberg state of NH*
K. Wang, J.A. Stephens, and V. McKoy
J. Chem. Phys. **93**, 7874 (1990)

15. *Orbital evolution and promotion effects in the photoionization dynamics of $^2\Sigma^-$ Rydberg states of OH*
J.A. Stephens and V. McKoy
J. Chem. Phys. **93**, 7863 (1990)

16. *Shape resonance effects in the rotationally resolved photoelectron spectra of $O_2$*
M. Braunstein, V. McKoy, S.N. Dixit, R.G. Tonkyn, and M.G. White
J. Chem. Phys. **93**, 5345 (1990)

17. *(2 + 1′) rotationally resolved resonance enhanced multiphoton ionization via the E $^2\Sigma^+$ (4s, 3d) and H $^2\Sigma$ (3d, 4s) Rydberg states of NO*
H. Rudolph and V. McKoy
J. Chem. Phys. **93**, 7054 (1990)

18. *Studies of valence photoionization of $Cl_2$*
M. Braunstein and V. McKoy
J. Chem. Phys. **92**, 4887 (1990)

19. *Cooper minima and rotationally resolved resonance enhanced multiphoton ionization spectroscopy*
H. Rudolph and V. McKoy
J. Chem. Phys. **91**, 7995 (1989)

20. *Multiple-specific shape resonance and autoionization effects in (2+1) resonance enhanced multiphoton ionization of $O_2$ via the d $^1\Pi_g$ state*
J.A. Stephens, M. Braunstein, and V. McKoy
J. Chem. Phys. **92**, 5319 (1990)

21. *Photoionization of the 3σ and 1 π orbitals of CH*
M.-T. Lee, J.A. Stephens, and V. McKoy
J. Chem. Phys. **92**, 536 (1990)

22. *Rotational branching ratios and photoelectron angular distributions in resonance enhanced multiphoton ionization of diatomic molecules*
K. Wang and V. McKoy
J. Chem. Phys. **95**, 4977 (1991)

23. *Ion rotational distributions at near-threshold photoelectron energies*
K. Wang, J.A. Stephens, and V. McKoy
Invited Paper in the Proceedings of the 10th
International Conference on VUV Radiation Physics
edited by Y. Petroff, I. Nenner, and F. Wuilleumier
(World Scientific, Singapore, 1992)

e. *Seminars and invited lectures presented on the studies outlined above include:*

1. Invited speaker at the Gordon Research Conference on Multiphoton Processes, June 1990, Colby-Sawyer Junior College, New Hampshire

2. Invited speaker at the European Research Conference on Very High Resolution Spectroscopy with Photoelectrons - ZEKE Spectroscopy, 28-31 October, 1991, Kreuth, Germany
   Note: The European Research Conferences are Gordon-like Research Conferences sponsored by the European Science Foundation and the Commission of the European Communities

3. Invited speaker at the 10th International Conference on Vacuum Ultraviolet Radiation Physics, 27-31 July, 1992, Paris, France

4. Invited speaker at the International Workshop on Photoionization, 24-28 August, 1992, Berlin, Germany. This is a *by invitation only* meeting covering significant developments in the field

5. Plenary speaker at the 1992 Sanibel Symposium on Photoinduced Phenomena, 13 March, 1992, St. Augustine, Florida

6. Colloquium speaker at the University of Nebraska, Lincoln, Nebraska, September, 1991

7. Colloquium speaker at Louisiana State University, Baton Rouge, Louisiana, Febraury, 1992

## 4. *Objectives of Proposed Research*

The broad objective of our proposed research is to continue and extend our theoretical studies of the rotational and vibrational distributions of ions resulting from resonance enhanced multiphoton ionization of molecules and molecular fragments and from single-photon ionization of these species by coherent UVV and XUV radiation. Our proposed studies of these ion distributions will provide both a robust description of key spectral features of interest in related experiments and needed insight into the underlying dynamics of these state-resolved photoelectron spectra. As in our studies to date, a major focus of our effort will be on joint theoretical and experimental studies of ion rotational distributions for resonance enhanced multiphoton ionization and single-photon ionization of a wide range of molecules. Specific objectives will include studies of ion rotational distributions for

REMPI and single-photon ionization of molecules and radicals such as $C\ell O$, BrO, $CC\ell$, $CH_2$, $CH_3$, $NH_3$, HCO, $H_2CO$, $C_2H_4$, $C_2H_5$, $C_6H_5$, and $C_6H_6$. Several of these molecules and radicals have been chosen on the basis of relevant technical applications and of their potential for providing insight into the underlying dynamics of ion rotational distributions in photoionization of polyatomic molecules. For example, $C\ell O$ and BrO radicals are of great interest due to their central role in the $C\ell O_x$ and $BrO_x$ cycles of stratospheric ozone depletion. Where feasible, our studies of these ion rotational distributions will be carried out jointly with experimental groups actively involved in measurements of such spectra. Our experience has shown how effective a strong interpleny between theory and experiment can be in analysis of these spectra, particularly for polyatomics.

Our proposed studies of ion rotational distributions for photoionization of many of the polyatomic molecules of interest, e.g., $C_2H_5$ and $C_6H_6$, will be significantly more demanding computationally than our studies to date of diatomic molecules and small polyatomic molecules such as $H_2O$. As discussed in sec. 2, the computationally significant requirement of our studies is the soluton of eq. (4) for the photoelectron orbitals $\Psi_{\mathbf{k}}^{(-)}$. In studies of ion rotational distributions at the low photoelectron energies of interest here, e.g., 50 meV, it is essential to use converged solutions of eq. (4) so as to faithfully represent the angular momentum coupling present in the molecular photoelectron wavefunction. To meet these computational needs we will develop and implement a strategy for doing these calculations on the Intel Delta System, a massively parallel supercomputer consisting of over 500 i860 microprocessors, each with 16 megabytes of memory and an observed performance of 3-5 megaflops, and a two-dimensional communication mesh. Such parallel supercomputers which achieve high aggregate speeds and massive memory by harnessing the power of commercially available microprocessors are particularly well suited for numerical solution of eq. (10) for the photoelectron orbitals for polyatomic ions.

The strategy for such a parallel implementation of our numerical procedure for obtaining these photoelectron orbitals would proceed as follows. The essential steps of this procedure are the generation of partial wave expansions of all quantities appearing in eq. (10) and the use of these partial wave expansions to numerically quadrature the matrix elements arising in this equation. These partial wave expansions are much more extensive for polyatomic ions than for linear systems. This can be readily seen from eq. (11) where for linear systems m must always be equal to m', i.e. projection of angular momentum along the molecular axis is a good quantum number, in any polyatomic molecule m' need not be equal to m. We hence have much more extensive changes in $\ell$ and m of the photoelectron as it scatters off a polyatomic ion cove. One can now simply distribute the

computational load of generating these partial wave expansions across the microprocessors and have these expansions proceed in parallel on the microprocessors. This step can be expected to be highly efficient since it is inherently parallel. Subsequent quadrature of the matrix elements which require manipulations and transformations of these partial wave expansions, which are now distributed over the microprocessors, can be achieved via a series of matrix multiplications. Based on the performance levels we have seen in our extensive use of the Intel Delta System in other applications[24] we expect to achieve very high computational speeds in the proposed applications. The resources of the Intel Delta System required for these studies are available to us.

## *References*


1. See, for example, M. Braunstein, V. McKoy, S.N. Dixit, R.G. Tonkyn, and M.G. White, J. Chem. Phys. **93**, 4345 (1990) ; R.T. Wiedemann, R.G. Tonkyn, M.G. White, K. Wang, and V. McKoy, J. Chem. Phys. **97**, 768 (1992)
2. W. Kong, D. Rodgers, and J.W. Hepburn, Proceedings of the 10th International Conference on Vacuum Ultraviolet Physics, edited by Y. Petroff, I. Nenner, and F. Wuilleumier (World Scientific, Singapore, 1992)
3. See, for example, R.G. Tonkyn and M.G. White, Rev. Sci., Instrum. **60**, 1245 (1989)
4. R. Wiedmann, M.G. White, K. Wang, and V. McKoy, J. Chem. Phys. (in press)
5. K. Müller-Dethlefs and E.W. Schlag, Ann. Rev. Phys. Chem. **42**, 109 (1991)
6. K. Wang and V. McKoy, J. Chem. Phys. **95**, 4977 (1991)
7. M.-T. Lee, K. Wang, and V. McKoy, J. Chem. Phys. **97**, 3108 (1992)
8. R.R. Lucchese, G. Raseev, and V. McKoy, Phys. Rev. A **25**, 2572 (1982)
9. R.R. Lucchese, K. Takatsuka, and V. McKoy, Phys. Rept. **131**, 147 (1986)
10. E. de Beer, M. Born, C.A. de Lange, and N.P.C. Westwood, Chem. Phys. Lett. **186**, 40 (1991)
11. K. Wang, J.A. Stephens, V. McKoy, E. de Beer, C. A. de Lange, and N.P.C. Westwood, J. Chem. Phys. **97**, 211 (1991)
12. E. de Beer, C.A. de Lange, J.A. Stephens, K. Wang, and V. McKoy, J. Chem. Phys. **95**, 714 (1991)
13. H. Rudolph and V. McKoy, J. Chem. Phys. **91**, 7995 (1989)

14. K. Wang and V. McKoy, J. Chem. Phys. **95**, 7872 (1991)

15. J. Xie and R.N. Zare, Chem. Phys. Lett. **159**, 399 (1989)

16. J. Xie and R.N. Zare (private communication)

17. J. Xie and R.N. Zare, J. Chem. Phys. **93**, 3033 (1990)

18. See, for example, E.R. Grant and M.G. White, Nature **354**, 249 (1991)

19. W. Kong, D. Rodgers, J.W. Hepburn, K. Wang, and V. McKoy, J. Chem. Phys. (to be published)

20. R.G. Tonkyn, R.T. Wiedmann, E.R. Grant, and M.G. White, J. Chem. Phys. **95**, 7033 (1991)

21. M.-T. Lee, K. Wang, V. McKoy, R.G. Tonkyn, R.T. Wiedmann, E.R. Grant, and M.G. White, J. Chem. Phys. **96**, 7848 (1992)

22. R.T. Wiedmann and M.G. White, Proceedings of the SPIE Optical Methods for Time - and State Resolved Chemistry,J **1638**, 273 (1992)

23. K. Wang, M.-T. Lee, V. McKoy, R.T. Wiedmann, and M.G. White, J. Chem. Phys. (to be published)

24. C. Winstead, P.G. Hipes, M.A.P. Lima, and V. McKoy, J. Chem. Phys. **94**, 5455 (1991)

## 5. *Scientific Training*

(a) Graduate students trained
Matthew Braunstein (1990)

(b) Degrees granted
Matthew Braunstein, Ph.D. (1990)

(c) Postdoctoral tenures
K. Wang (1990-92)

## 6. *Federal Support for Overall Research Program*

1. Air Force Office of Scientific Research ($79,635, 6/1/92 - 5/31/93)

2. National Science Foundation ($88,200, 3/11/92 - 2/28/93)